

UNIVERSIDAD SAN FRANCISCO DE QUITO USFQ
Colegio de Ciencias e Ingeniería

**Anomalous SPASER Emission in Gain Enhanced
Silver Nanoshells**

Proyecto de Investigación

Karen Gabriela Caicedo Santamaría

Física

Trabajo de titulación presentado como requisito para la obtención
del título de Licenciada en Física

Quito, 28 de mayo de 2018

UNIVERSIDAD SAN FRANCISCO DE QUITO USFQ
Colegio de Ciencias e Ingeniería

**HOJA DE CALIFICACIÓN DE TRABAJO DE
TITULACIÓN**

**Anomalous SPASER Emission in Gain Enhanced Silver
Nanoshells**

Karen Gabriela Caicedo Santamaría

Calificación:

Nombre del profesor, Título académico: Alessandro Veltri, Ph.D.

Firma del profesor

.....

Quito, 28 de mayo de 2018

Derechos de Autor

Por medio del presente documento certifico que he leído todas las Políticas y Manuales de la Universidad San Francisco de Quito USFQ, incluyendo la Política de Propiedad Intelectual USFQ, y estoy de acuerdo con su contenido, por lo que los derechos de propiedad intelectual del presente trabajo quedan sujetos a lo dispuesto en esas Políticas. Asimismo, autorizo a la USFQ para que realice la digitalización y publicación de este trabajo en el repositorio virtual, de conformidad a lo dispuesto en el Art. 144 de la Ley Orgánica de Educación Superior.

Firma del estudiante
Nombres y apellidos:	Karen Gabriela Caicedo Santamaría
Código:	00122844
Cédula de Identidad:	1722636741
Lugar y fecha:	Quito, 28 de mayo de 2018

Dedicado a mi madre

Agradecimientos

Agradezco a Dios por darme fuerzas en este camino, por lo mucho que aprendí gracias a él. Agradezco a mi madre porque ha sido un apoyo incondicional para mí y siempre está dispuesta a ayudarme. Agradezco a mis abuelitos por su inmenso amor y su dulzura que me ayudaban a sobrellevar los problemas. Agradezco a Alessandro por toda la paciencia que tuvo conmigo y por regalarme no solo su conocimiento sino su amistad, a Ashod por darme la oportunidad de trabajar en este proyecto. Agradezco a Dario por siempre haberme escuchado y ser un gran tutor.

Agradezco al resto de mi familia por estar conmigo siempre. Agradezco a María Gracia, Katherine y Carlita por ser como mis hermanas y confiar en mí ciegamente. Agradezco a Roberto, Pablito, Jorge, Felipe y mis demás amigos por estar a mi lado durante este tiempo y compartir tantas experiencias. Agradezco a Fernando por darme fuerzas y sostener mi mano a pesar de cuán duro se vea el camino.

Resumen

En el presente trabajo de investigación, se describe el comportamiento de una nanoestructura conformada por un cascarón metálico en cuyo centro se encuentra un medio de ganancia que compensa las pérdidas de energía del sistema. A partir de un sistema de ecuaciones dinámicas que dan forma al sistema, se obtienen dos resultados que contrastan. El primero se deduce a partir de un tratamiento analítico de las ecuaciones donde se observa una línea de emisión para una frecuencia de SPASER determinada en el estado estacionario. El segundo resultado surge del tratamiento numérico de las ecuaciones; la evolución en el tiempo del sistema sugiere que no se alcanza el estado estacionario y la emisión de intensidades no se da para una sola frecuencia sino para un rango de frecuencias estrecho en el resultado dinámico obtenido.

Abstract

In the present research work, we discuss the behavior of a nanostructure conformed by a metallic spherical shell whose core is filled by a gain material to compensate the energy losses of the system. From a set of dynamic equations that describe to the system, two contrasting results are obtained. The first is deduced from an analytical treatment of the equations where a LASER like emission line is observed for a precise frequency suggesting the existence of the controversial SPASER phenomenon. The second result arises from the numerical treatment of the equations; the time evolution of the system suggests that the steady state is never reached and the emission of intensities is not given for a single frequency but for a narrow range of frequencies in the obtained dynamical result.

Contents

List of figures	9
1 Introduction	10
1.1 Brief Overview of Nanotechnology	10
1.2 Plasmonics	11
1.3 Goals of the Present Work	12
2 Plasmonics and Spasers	13
2.1 Diffraction Limit	13
2.2 Surface Plasmons	16
2.3 Localized Surface Plasmons	17
2.4 Optical Gain Materials as Loss-Compensators	19
2.5 Surface Plasmon Amplification by Stimulated Emission of Radiation (SPASER)	19
3 Theoretical Model	21
3.1 System Description	21
3.1.1 Gain Material	22
3.1.2 Metal	24
3.2 The Shape of the System	25
4 Results	28
4.1 Steady State and Spasing Condition	28
4.2 Dynamical Result	31
4.3 Conclusions	33
Appendices	35
A Gain Medium Electric Permittivity	36
B Transition Frequency Condition	39
References	40

List of Figures

1.1	Lycurgus cup. Left hand side: light source located outside the goblet; right hand side: light source located inside the goblet	12
2.1	Propagation of surface plasmon polaritons at a matallic surface [Wikimedia Commons, 2013].	15
2.2	Mechanism to excite SPPs through a prism. Left: Turbadar-Kretschmann-Raether configuration. Right: Turbadar-Otto configuration. [20] . .	16
2.3	Metallic nanoparticle impinged by an electric field in the quasi-static approximation [22]	17
3.1	Nanoshell system: optical gain material inside the core and a silver shell in a dielectric solvent.	21
4.1	Time evolution of the system when $\epsilon_h^{''th}(\omega_{sp}) = \epsilon_h''(\omega_{21})$	32
4.2	Time evolution of the system when $\epsilon_h^{''th}(\omega_{sp}) > \epsilon_h''(\omega_{21})$	33

Chapter 1

Introduction

1.1 Brief Overview of Nanotechnology

Nanotechnology is a young branch of physics concerned with taking advantage of physical, chemical and biological processes in a nanometric scale (< 100 nm) with the purpose of develop technology within molecular sizes, and create devices and machines in this scale. The scientific definition states nanotechnology is the application of technology in the gap between classical and quantum mechanics [7]. The idea of exploring nanoscale solutions was presented for the first time by Richard Feynman in 1959 during a prophetic lecture he presented to the American Physical Society; in which he actually predicted some technological advances that nowadays are a reality, such as writing huge amounts of information in small areas by using electron microscopes [6]. However, in his speech Feynman didn't used the word "nanotechnology", which was coined by Norio Taniguchi in 1974 during a talk about how the dimensional accuracy with which we make things had enhanced in the course of time [6]. In the current times, we can affirm that nanoscale advances are shaping our world: nanotechnology is in fact already present in semiconductor industries, automotive and medical fields, and computing and communication technology industries.

The importance of nanotechnology not only in the enormous variety of applications in which is currently used, but also in its potential to allow technological advances that were not even thinkable few decades ago [7]. Such as nanosorbents, nanocatalysts, bioactive nanoparticles, nanostructured catalytic membranes just to mention some, moreover nanoparticle enhanced filtration are possible solutions,

nowadays studied, to improve water quality and make it drinkable [9]. Nanotechnology is also involved in the increase in agricultural production; nanosensors are now produced to detect microbes, toxic pollutants and humidity; semiconductor nanostructures are used in the process of degrading organic pesticides and industrial pollutants [10]. Finally, one of the most important application of nanotechnology is in cancer therapy; semiconductor quantum dots and iron oxide nanocrystals can in fact be used to target tumor antigens and tumor vasculatures when linked with tumor targeting ligands [11].

1.2 Plasmonics

The study of the local fields at the interface between a metal and a dielectric is a growing part of nanophotonics which is of course included in the vast field of nanotechnology. In the year 2000, the California Institute of Technology coined the word “plasmonics” to describe this promising branch of physics [12]. One of the main interest in the study of plasmonics is its capability to generate a confinement of the electromagnetic fields in regions smaller than the wavelength [8].

The importance of developing photonic devices lies in the optimization of data transport and communication. Optical fiber is a good example of those technological photonic advances since it is an effective light signals guide. While the use of light has a lot of advantages, its fast and reliable, and it doesn't produce much heat; it has a problem of scalability: the diffraction limit. This wall forced scientists to look for a new way to transport optical signals through nanometric devices. In the 1980s, scientists experimentally demonstrated that, at the interface between a metal and a dielectric, a resonant interaction can be reached between directed light waves and conductive electrons at the surface of the metal; of course, this is only possible if the system is submitted to the right conditions [12].

While it is now easy to think about plasmonics as one of the pillars of cutting edge nanotechnology, it is also worth noting that has been present in human inventions way before the term was even coined. In fact, humans have taken advantage of photonic effects since immemorial times without even realizing it. One of the most famous and ancient devices created by using metallic impurities is the Lycurgus cup: a Roman goblet that, through plasmonic excitation of the electrons in the metallic particles, acquires a green tone when scatters light coming from a source localized outside the goblet, and has a red tinge when the light source is placed within it because the glass transmits only the longer wavelengths while

absorbs the shorter ones [12]. Figure 1.1 shows the Lycurgus cup, now exhibited in the British Museum.



Figure 1.1: Lycurgus cup. Left hand side: light source located outside the goblet; right hand side: light source located inside the goblet

A deeper explanation of plasmonics will be used to introduce some basic concepts of plasmonics in the following chapter.

1.3 Goals of the Present Work

The purpose of the present work is to make a theoretical description of the plasmonic response of a metallic nanoshell embedding an externally pumped active gain material. We are specially interested in the search of a spaser regime and the conditions for which it occurs, as well as the search of a steady state of the optical properties of this structure. The system studied is exemplified by considering the metal to follow the classical Drude model, and by modeling the gain material as a two-level system of continuum emitters in a thermal bath.

Chapter 2

Plasmonics and Spasers

2.1 Diffraction Limit

In 1873, Ernst Abbe deduced there is a limit in the resolution of optical imaging instruments, what is called the diffraction limit [2]. It states is not possible to focus light in objects whose length is smaller than approximately one half of the wavelength of the incident light (200 nm) [13]. Abbe determined that the diffraction for a microscope limit is

$$d = \frac{\lambda}{2\eta \sin \theta}, \quad (2.1)$$

where λ is the wavelength of the light beam, η is the refraction index of the medium, and θ is the angle on incidence [14]. More generally, Heisenberg uncertainty principle, i.e. $\Delta p_x \Delta x \geq \hbar/2$, applied to incident photons, enables us to state a relation between the wavelength of the light and the spatial confinement of the observed object. The momentum of a photon is $p_x = \hbar k_x$.

$$\Delta x \geq \frac{1}{2\Delta k_x} \quad (2.2)$$

The maximum possible spread in the wavevector k_x is $2\pi/\lambda$, thus we can deduce the following expression:

$$\Delta x \geq \frac{\lambda}{4\pi}. \quad (2.3)$$

Equation 2.3 shows that, for visible light (500 nm), is not possible to observe an object that is smaller than about 200 nm. Nevertheless, in recent times different methods have emerged to surpass the diffraction limit.

We are specially interested in the method that uses surface plasmons. The modus operandi of surface plasmons is the following: equation 2.2 conveys the spatial confinement in a given direction depends inversely on the spread of the component of the wavevector in the same direction. In order to decrease Δx , we need to find a way to increase the spread of the wavevector component of interest, for instance k_x .

This goal can be achieved by increasing k_x to values beyond the total wavevector, and making purely imaginary the two perpendicular components, in this case k_y and k_z ; this allows us to keep the magnitude of the total wavevector as $2\pi/\lambda$. Since the k_x component is increased, its spread also grows and equation 2.3 is fulfilled. However, there is an implication caused by the increase of confinement: if we insert the imaginary part of the wavevector into the plane wave equation, the behavior of the field in \hat{z} will be $e^{ik_z z} = e^{-|k_z|z}$. This expression shows that in one direction of z , the field decays exponentially while, in the opposite direction, it increases exponentially. The last kind of field has no physical meaning, so we can dismiss it in order to let equation 2.3 always valid in free space [13]. The physical meaning of this is that on a metal-dielectric interface, surface plasmons polaritons (SPPs) are evanescent waves [8].

From Maxwell's equations, SPPs wavevector components at the interface between the metal and the dielectric are described by equations 2.4 and 2.5, and are functions of the relative permittivities of the two materials involved. If $\epsilon_1(\omega)$ represents the relative electric permittivity in the metal, and ϵ_2 is the relative permittivity of the dielectric, we can write for k_x^2 and $k_{y,z}^2$ the following expressions:

$$k_x^2 = k_0^2 \frac{\epsilon_1(\omega)\epsilon_2}{\epsilon_1(\omega) + \epsilon_2}, \quad (2.4)$$

$$k_{y,z}^2 = k_0^2 \frac{\epsilon_j^2}{\epsilon_1(\omega) + \epsilon_2}, \quad (2.5)$$

where we used $k_0 = \omega/c$. $j = 1$ gives $k_{y,z}$ in the dielectric, while $j = 2$ gives $k_{y,z}$ in the metal.

Let's now discuss a bit more in detail how an imaginary value for some components of the wavevector can be experimentally achieved. In the case of metals, the real part of ϵ_1 is negative for determined values of frequency; while for a conductor without attenuation, i.e. a superconductor, the conditions that allow to have a purely real k_x and imaginary $k_{y,z}$ are [8]:

$$\epsilon_1(\omega)\epsilon_2 < 0, \quad (2.6a)$$

$$\epsilon_1(\omega) + \epsilon_2 < 0. \quad (2.6b)$$

Since it is still difficult to operate with superconductors due to the conditions they require to exist, scientists are interested in work with metals. Moreover, at the interface between a metal and a dielectric, oscillations described by equations 2.4 and 2.5 takes place. At this point is important to note that surface plasmon frequency ω_{sp} is an upper limit for the frequencies that satisfies the set of equations 2.6. Then, surface plasmons will appear below this limit.

Figure 2.1 shows how occurs the propagation of surface plasmon polaritons at a matallic surface.

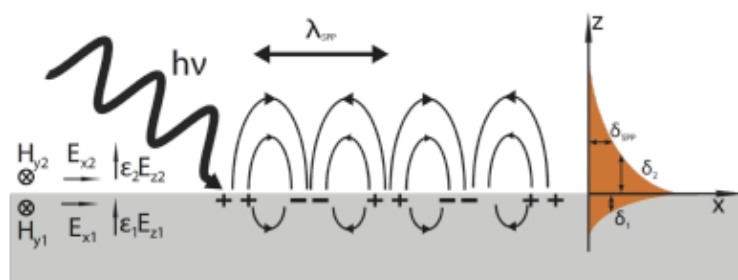


Figure 2.1: Propagation of surface plasmon polaritons at a matallic surface [Wikimedia Commons, 2013].

2.2 Surface Plasmons

As discussed in the previous paragraph, surface plasmons are defined as charge oscillations that take place at the interface of a conductor and a dielectric [15]. However, the first historical record of the term occurred not before 1956, when David Pines realized there are energy losses of electrons whose motion occurs at the surface of metals; in this work, Pines coined the name plasmon to describe quasiparticles that emerge from the quantization of plasma oscillations [16, 2]. In 1957, while Rufus Richtie was studying energy losses of electrons laying on metallic thin films, he concluded plasmon modes can take place near the surface of metals [2, 17].

The surface plasmon polariton quasiparticle is defined when there is a dielectric above the surface of a metallic nanoparticle. The quantum of polarization in the dielectric material is what we call polariton.

While the possibility of SPP was theoretically demonstrated up to this point, it was not possible to excite SPPs experimentally in metallic surfaces until in 1968 Andreas Otto, Erich Kretschmann and Heinz Raether designed a way to excite plasmons by using a prism with high refractive index localized close to the interface between metal and vacuum; these conditions create an evanescent wave due to the frustrated total reflection produced by the prism [18, 19]. Figure 2.2 exhibit the mechanism of action of the prism and the creation of SPP waves.

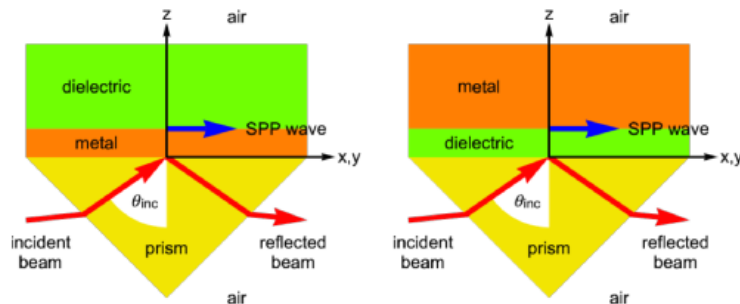


Figure 2.2: Mechanism to excite SPPs through a prism. Left: Turbadar-Kretschmann-Raether configuration. Right: Turbadar-Otto configuration. [20]

2.3 Localized Surface Plasmons

In this paragraph we will focus on the Localized surface plasmons (LSPs) which are the most directly related to the subject of our study. LSPs are “non-propagating excitations of the conduction electrons of metallic nanostructures coupled to an electromagnetic field” [8]. Uwe Kreibig and Peter Zacharias studied for the first time LSP, specifically they described the optical properties of metallic nanoparticles through surface plasmons [2, 21]. It is worth mentioning that the non-propagating resonance of LSPs is caused by an effective restoring force exerted in the conduction electrons as a consequence of the curved shape of the nanoparticle. The advantage of LSPs over SPPs is that they can be excited by using direct incident light; there is no necessity of a prism, which is the case of SPPs [8].

Localized surface plasmons are studied through the interaction of a metallic nanoparticle, immersed in a dielectric, with an external electric wave. As a result of this interplay, a resonance condition will appear in the local electromagnetic fields around the nanoparticle.

Quasi-static approximation allows us to describe the interaction between the metallic nanoparticle and the incident electric field provided that $a \ll \lambda$, where a is the radius of the nanoparticle and λ is the wavelength of the electromagnetic field [8]. If this condition is fulfilled, then we can consider the external electric field as uniform in space, $\mathbf{E}_0 = E_0 \hat{z}$.

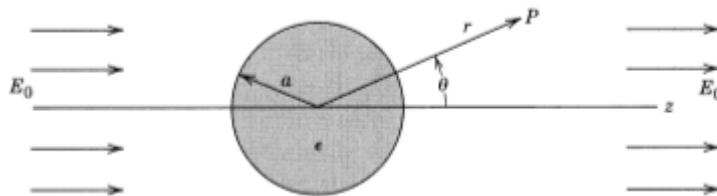


Figure 2.3: Metallic nanoparticle impinged by an electric field in the quasi-static approximation [22]

This allows us to use an electrostatic approach: $\nabla \times \mathbf{E} = \mathbf{0}$, this means that we can deduce we can deduce the electric potential ϕ as a solution of the Laplace equation: $\nabla^2 \phi = 0$. Then applying the boundary conditions, we obtain that the electric potential outside the nanoparticle has a dipolar shape described by the expression:

$$\phi_{out} = -E_0 r \cos \theta + \frac{\mathbf{p} \cdot \hat{\mathbf{r}}}{4\pi\epsilon_0\epsilon_d r^2}, \quad (2.7)$$

where \mathbf{p} is the dipole moment of the nanoparticle and ϵ_d is the relative permittivity of the dielectric, while \mathbf{p} is given by

$$\mathbf{p} = 4\pi\epsilon_0\epsilon_d a^3 \frac{\epsilon_m(\omega) - \epsilon_d}{\epsilon_m(\omega) + 2\epsilon_d} \mathbf{E}_0, \quad (2.8)$$

where $\epsilon_m(\omega)$ is relative permittivity of the metallic nanoparticle. The proportionality term is often referred as the polarizability of the particle, α : it is worth noting that this expression has the form of the Clausius-Mossotti relation [22].

$$\alpha(\omega) = 4\pi\epsilon_0\epsilon_d a^3 \frac{\epsilon_m(\omega) - \epsilon_d}{\epsilon_m(\omega) + 2\epsilon_d} \quad (2.9)$$

To determine the polarizability is relevant because from it one can determine important quantities such as coefficients of scattering, absorption, extinction, etc [23]. Observe that the polarizability depends on the size of the particle so, as we already said, this result is valid only when the quasi-static limit is satisfied. For bigger particles, the Mie theory has to be used. Since the relative permittivity of a metal is a complex function of frequency, as shown in Drude model, i.e. equation 2.10,

$$\epsilon_m(\omega) = 1 - \frac{\omega_p^2}{\omega(\omega + i\gamma)}, \quad (2.10)$$

where ω_p is the plasmon frequency and λ is the collision frequency, the polarizability is a complex function of the frequency as well. Note that when $\gamma \ll \omega$, a singularity is reached when $\epsilon_m(\omega_0) = -2\epsilon_d$, known as the Fröhlich condition, which is the resonant condition we briefly mentioned in the beginning. For conductors without attenuation ($\lambda = 0$) or in the high frequency regime is possible to achieve the singularity. However, real metals have non-negligible damping, i.e. the imaginary positive part of its relative permittivity bring with it losses. Which means that also the imaginary part of the polarizability is larger than zero, implying dispersion of energy in the medium [2]. Fortunately, there are few suggestions

to compensate these losses. In the following section, we discuss a compensation method in order to restore a LSP resonance behavior without losses.

2.4 Optical Gain Materials as Loss-Compensators

Since the source of the losses is the imaginary positive component of the relative electric permittivity of the metal, then we need to add something with a negative imaginary part in the relative permittivity. An encouraging method is by using active compounds externally pumped capable to transfer energy to the metal, such as optical gain materials [5]. Some examples of optical gain material are quantum dots and fluorescent molecules [24]. Gain materials injects energy to the system by transitions from high energy states to low energy states; only possible when population inversion takes place, this means when the majority of the quantum elements lays in the higher energy state [2].

Optical gain materials has a complex permittivity dependent on the frequency, $\epsilon_g(\omega)$. In the steady state, $\epsilon_g(\omega)$ has a “single Lorentzian emission line shape” [5], as shown in the following expression,

$$\epsilon_g(\omega) = -\frac{\epsilon_g''(\omega_g)\Delta}{2(\omega - \omega_g) + i\Delta}, \quad (2.11)$$

where ω_g is the gain frequency and the center of the Lorentzian. $\epsilon_g(\omega)$ has a negative imaginary contribution, then it allows us to compensate the loss caused by the imaginary part of the permittivity of the metal.

2.5 Surface Plasmon Amplification by Stimulated Emission of Radiation (SPASER)

In 2003, Bergman and Stockman demonstrated the possible existence of high-intensity line emissions on selected surface plasmon modes taking place in nanoscale structures; all this by a quantization of the surface plasmon fields and the stimulated emission produced by them [25]. Stockman also explains a solution to compensate the losses that arise when a noble metal interacts with an incident

optical frequency field; i.e. by using gain material described by the optical-Bloch formalism, which makes way for a second quantization of the surface plasmon field. The Hamiltonian related with this kind of systems portrays the creation and destruction of surface plasmon modes through ladder operators. It also has two more contributions that has to do with the energy of the gain material and the coupling of the electric field with the dipolar moment of each gain dot [2].

$$H = \hbar \sum_n \omega_n a_n^\dagger a_n + H_g - \sum_p \mathbf{E}(\mathbf{r}_d) \cdot \mathbf{d}^{(p)} \quad (2.12)$$

In other words, a SPASER is a line emission of intensity that occurs for only one frequency. We are specially interested in this concept since the nanoshell system we study is assisted by a gain material, so SPASER phenomenon would appear.

Chapter 3

Theoretical Model

3.1 System Description

The system studied in the present work consists of a silver nanoshell, which have its core filled with an optical gain material that can be pumped from an external power source. We will build a model which allows the plasmonic field to be excited through an external electromagnetic probe field, then we will look for emissive SPASER solutions that should occur when this field is put to zero. Figure 3.1 exhibit the system structure object of this study.

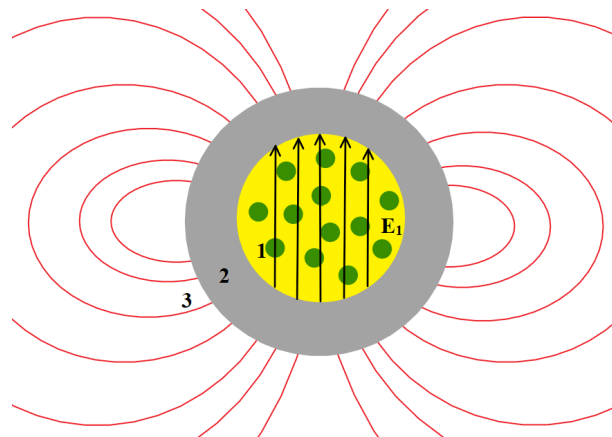


Figure 3.1: Nanoshell system: optical gain material inside the core and a silver shell in a dielectric solvent.

The inner region (1) is a sphere of radius a_1 , and it's made of two components: a background dielectric whose permittivity, ϵ_b , is constant, in our case, silica; and an optical gain material whose permittivity is complex and is frequency dependent, $\epsilon_g(\omega)$. Giving rise to a two contribution permittivity which we will denote as $\epsilon_h(\omega)$. Region (2) is a silver shell whose outer radius is a_2 , and its permittivity, $\epsilon_m(\omega)$, is also frequency dependent. Region (3) is made of a dielectric solvent with constant permittivity, ϵ_3 , for which we used water.

3.1.1 Gain Material

Active medium is treated as a two-level system of continuum emitters in a thermal bath using the density matrix formalism and the optical Bloch equations [4].

$$\frac{d\rho_{21}}{dt} - \left(i\omega_{21} - \frac{1}{\tau_2} \right) \rho_{12} = \frac{iN\boldsymbol{\mu} \cdot \mathbf{E}_1}{\hbar} \quad (3.1)$$

$$\frac{dN}{dt} + \frac{N - \tilde{N}}{\tau_1} = \frac{2i(\rho_{12} - \rho_{21})\boldsymbol{\mu} \cdot \mathbf{E}_1}{\hbar} \quad (3.2)$$

The i,j element of the density matrix is represented by ρ_{ij} , $N = \rho_{22} - \rho_{11}$. τ_1 and τ_2 are constants that describe relaxation processes related to phase and energy due to the interaction with the thermostat. ω_{21} is the transition frequency between energy levels 2 and 1, and the term $\boldsymbol{\mu} \cdot \mathbf{E}_1$ represents the non-radiative coupling to the metal where $\boldsymbol{\mu}$ is the transition dipole moment. $\tilde{N} = \frac{W\tilde{\tau}_1 - 1}{W\tilde{\tau}_1 + 1}$ is the population inversion caused by the pump, W is the phenomenological pump rate, and $\tilde{\tau}_1$ is a relaxation constant. The radiative contribution is incorporated in equation 3.2 through τ_1 .

The polarization density of the gain material contributes to the polarization density of region (1), \mathbf{P}_1 .

$$\mathbf{P}_1 = \epsilon_0\chi_b\mathbf{E}_1 + \frac{n_g}{4\pi} \int_0^{4\pi} (\rho_{12} + \rho_{21}) \boldsymbol{\mu} d\Omega \quad (3.3)$$

where χ_b is the susceptibility of the background of the dielectric host, n_g is the density of gain molecules, and $d\Omega$ is the solid angle differential. For the sake of simplicity, we define the following field

$$\mathbf{\Pi} = \frac{n_g}{4\pi} \int_{\Omega} \rho_{12} \boldsymbol{\mu} d\Omega \quad (3.4)$$

The density matrix is hermitian, i.e. $\rho_{mn} = \rho_{nm}^*$, thus the polarization density can be written as

$$\mathbf{P}_1 = \epsilon_0 \chi_b \mathbf{E}_1 + \frac{n_g}{4\pi} \int_0^{4\pi} (\rho_{12} + \rho_{12}^*) \boldsymbol{\mu} d\Omega = \epsilon_0 \chi_b \mathbf{E}_1 + \mathbf{\Pi} + \mathbf{\Pi}^* \quad (3.5)$$

An integration of equations 3.1 and 3.2 over the solid angle allow us to restate them.

$$\frac{d\mathbf{\Pi}}{dt} - \left(i\omega_{21} - \frac{1}{\tau_2} \right) \mathbf{\Pi} = \frac{in_g \mu^2}{3\hbar} N \mathbf{E}_1 \quad (3.6)$$

$$\frac{dN}{dt} + \frac{N - \tilde{N}}{\tau_1} = \frac{2i}{\hbar n_g} (\mathbf{\Pi} - \mathbf{\Pi}^*) \cdot \mathbf{E}_1 \quad (3.7)$$

We are dealing with optical fields so we will be looking for solutions of the form:

$$\mathbf{\Pi} = \tilde{\mathbf{\Pi}}(t) e^{i\omega t}, \quad (3.8a)$$

$$\mathbf{E}_1 = \frac{1}{2} \left[\tilde{\mathbf{E}}_1(t) e^{-i\omega t} + \tilde{\mathbf{E}}_1^*(t) e^{i\omega t} \right], \quad (3.8b)$$

$$\mathbf{P}_1 = \frac{1}{2} \left[\tilde{\mathbf{P}}_1(t) e^{-i\omega t} + \tilde{\mathbf{P}}_1^*(t) e^{i\omega t} \right], \quad (3.8c)$$

which, once substituted in equations 3.6 and 3.7 gives us the following system of equations.

$$\frac{d\mathbf{\Pi}}{dt} + \left[i(\omega - \omega_{21}) + \frac{1}{\tau_2} \right] \mathbf{\Pi} = \frac{in_g\mu^2}{6\hbar} N\mathbf{E}_1^* \quad (3.9a)$$

$$\frac{dN}{dt} + \frac{N - \tilde{N}}{\tau_1} = -\frac{2\Im[\mathbf{E}_1 \cdot \mathbf{\Pi}]}{n_g\hbar} \quad (3.9b)$$

$$\mathbf{P}_1 = \epsilon_0\chi_b\mathbf{E}_1 + 2\mathbf{\Pi}^* \quad (3.9c)$$

Observe that we deleted the tildes from every field, then the equations are equations of the envelopes of the fields, which are the physically relevant quantities.

The gain medium has a frequency dependent permittivity, $\epsilon_g(\omega)$, which, in the steady state, is described with a “single Lorentzian emission line shape” centered at the gain frequency ω_{21} [5].

$$\epsilon_g(\omega) = -\frac{\epsilon_g''(\omega_{21})\Delta}{2(\omega - \omega_{21}) + i\Delta} \quad (3.10)$$

3.1.2 Metal

The interaction between each electron inside the metal and the electric field \mathbf{E}_2 causes a displacement \mathbf{r} of the electron from its equilibrium position. This phenomenon is described by the free electron model, as shown in the following differential equation

$$\frac{d^2\mathbf{r}}{dt^2} + 2\gamma\frac{d\mathbf{r}}{dt} = \frac{e}{m_e}\mathbf{E}_2, \quad (3.11)$$

where γ is the collision frequency between the electrons, e is the elementary charge, and m_e is the electron’s mass. The polarization density in the metal is $\mathbf{P}_2 = n_e e\mathbf{r}$, where n_e is the density of electrons in the metal; thus, equation 3.11 allows us describe the time evolution of P_2 as follows

$$\frac{d^2\mathbf{P}_2}{dt^2} + 2\gamma\frac{d\mathbf{P}_2}{dt} = \epsilon_0\omega_p\mathbf{E}_2, \quad (3.12)$$

where $\omega_p = n_e e^2 / m_e \epsilon_0$. As we did before, we will be looking for oscillating solutions for \mathbf{E}_2 and the polarization density \mathbf{P}_2 :

$$\mathbf{E}_2 = \frac{1}{2} \left[\tilde{\mathbf{E}}_2(t) e^{-i\omega t} + \tilde{\mathbf{E}}_2^*(t) e^{i\omega t} \right] \quad (3.13)$$

$$\mathbf{P}_2 = \frac{1}{2} \left[\tilde{\mathbf{P}}_2(t) e^{-i\omega t} + \tilde{\mathbf{P}}_2^*(t) e^{i\omega t} \right] \quad (3.14)$$

Again, we take the second time derivative of the slowly varying polarization densities to be neglected and we drop the tildes. Equation 3.14 becomes

$$\frac{d\mathbf{P}_2}{dt} - \frac{\omega^2 + 2i\gamma\omega}{2(\gamma - i\omega)} \mathbf{P}_2 = \frac{\epsilon_0 \omega_p^2}{2(\gamma - i\omega)} \mathbf{E}_2 \quad (3.15)$$

Observe that in the steady state, i.e. $d\mathbf{P}_2/dt = \mathbf{0}$, \mathbf{P}_2 has a linear dependence with \mathbf{E}_2 . This means the metal acts as a linear material, $\mathbf{P}_2 = \epsilon_0 (\epsilon_m - 1) \mathbf{E}_2$. The steady state metal permittivity is illustrated by the classical Drude model [3].

$$\epsilon_m(\omega) = 1 - \frac{\omega_p^2}{\omega(\omega + i\gamma)} \quad (3.16)$$

3.2 The Shape of the System

As already mentioned, we are going to consider there is a probe field \mathbf{E}_0 outside the nanoshell system, also we will consider the size of the nanoshell is much smaller than the wavelength of the probe field. This will allow us to work in the quasi-static limit, which is equivalent to consider the speed of light to travel in zero time through our system. This approximation is solid for particles of 10-20 nm of radius, but begins to fall apart for particles bigger than 60-100 nm. Electric displacement \mathbf{D} allows us to describe the electric field and the polarization of the system without the necessity of assuming a specific gauge. Since there are no free charges in the system, then the divergence of \mathbf{D} is zero in every region.

$$\nabla \cdot \mathbf{D} = 0 \quad (3.17)$$

Quasi-static limit enables us to consider as irrotational the electric field, and it implies that exists a potential ϕ such that $\mathbf{E} = -\nabla\phi$. In the structure and the conditions we are considering, it is possible to show that also the polarization \mathbf{P} is irrotational, allowing us to define two scalars ψ_1 and ψ_2 such that $\mathbf{\Pi} = -\nabla\psi_1$ and $\mathbf{P}_2 = -\nabla\psi_2$. Now, from this it naturally follows that as $\mathbf{D} = \epsilon_0\mathbf{E} + \mathbf{P}$, \mathbf{D} is also irrotational. Besides, since there are no free charges in the system, the divergence of the electric displacement is zero, what means that ϕ , ψ_1 and ψ_2 follows Laplace's equation, $\nabla^2\Phi = 0$, whose solution is of the form

$$\Phi_{1,2,3} = \sum_{l=0}^{\infty} \left[\tilde{p}_l^{(1,2,3)} r^l + \frac{p_l^{(1,2,3)}}{r^{l+1}} \right] P_l(\cos\theta). \quad (3.18)$$

The functional form of the electric potential in this structure is well known in literature and Andrés Cathey, on his work Spaser Instability in Gain-Assisted Silver Nanoshell [2], made the calculations for the polarization potentials by using equation 3.18. The complete set for the potentials of both the field and the polarization is:

$$\phi_1(r, \theta, t) = \left[\frac{p^{(2)}}{\rho^3 a_2^3} + \frac{p^{(3)} - p^{(2)}}{a_2^3} - E_0 \right] r \cos\theta, \quad (3.19a)$$

$$\phi_2(r, \theta, t) = \left[\frac{p^{(3)} - p^{(2)}}{a_2^3} - E_0 \right] r \cos\theta + p^{(2)} \frac{\cos\theta}{r^2}, \quad (3.19b)$$

$$\phi_3(r, \theta, t) = -E_0 r \cos\theta + p^{(3)} \frac{\cos\theta}{r^2}, \quad (3.19c)$$

$$\psi_1(r, \theta, t) = q^{(1)} r \cos\theta, \quad (3.19d)$$

$$\psi_2(r, \theta, t) = q^{(2)} r + \sigma \frac{\cos\theta}{r^2}. \quad (3.19e)$$

These were included by Andrés on the dynamical equations describe the system, 3.9a, 3.9b and 3.15. Then, the equations were normalized in order to make them dimensionless: $\sigma \rightarrow \sigma/\epsilon_0\rho^3 a_2^3$, $t \rightarrow \omega_p$, $\omega \rightarrow \omega/\omega_p$, $p_2 = p^{(2)}/\rho^3 a_2^3$, $p_3 = p^{(3)}/a_2^3$, $q_1 = q^{(1)}/\epsilon_0$, and $q_2 = q^{(2)}/\epsilon_0$.

$$\frac{dq_1}{dt} + \left[i(\omega - \omega_{21}) + \frac{1}{\tau_2} \right] q_1 = \frac{iN\epsilon_h''(\omega_{21})}{2\tau_2} [E_0^* - p_3^* - (1 - \rho^3)p_2^*], \quad (3.20a)$$

$$\frac{dN}{dt} + \frac{N - \tilde{N}}{\tau_1} = \Im\{q_1 [E_0 - p_3 - (1 - \rho^3)p_2]\}, \quad (3.20b)$$

$$\frac{dq_2}{dt} - \frac{i\omega}{\omega^2(1 - \epsilon_m) + 1} q_2 = -\frac{i\omega(1 - \epsilon_m)}{\omega^2(1 - \epsilon_m) + 1} [E_0 - p_3 + \rho^3 p_2], \quad (3.20c)$$

$$\frac{d\sigma}{dt} - \frac{i\omega}{\omega^2(1 - \epsilon_m) + 1} \sigma = \frac{i\omega(1 - \epsilon_m)}{\omega^2(1 - \epsilon_m) + 1} p_2, \quad (3.20d)$$

$$(3.20e)$$

Moreover, by using boundary conditions on the radial components of the electric field and the polarization, Andrés found expressions for p_2 and p_3 . $\epsilon_h''(\omega_{21}) = -\frac{2n\tilde{N}\mu^2}{3\hbar\Delta}$ and $\Delta = \frac{2}{\tau_2}$ were also defined, where $\epsilon_h''(\omega_{21})$ is the imaginary component of the permittivity in the core, ϵ_h .

$$p_2 = \frac{(\epsilon_b - 1)(E_0 - p_3) + q_2 - 2(q_1^* + \sigma)}{\epsilon_b + 2 - \rho^3(\epsilon_b - 1)}, \quad (3.21a)$$

$$p_3 = \frac{[(1 - \epsilon_3)(\epsilon_b + 2) + \rho^3(\epsilon_b - 1)(\epsilon_3 + 2)] E_0 - 6\rho^3 q_1^* - (1 - \rho^3) [(\epsilon_b + 2)q_2 - 2\rho^3(\epsilon_b - 1)\sigma]}{(\epsilon_b + 2)(1 + 2\epsilon_3) + 2\rho^3(\epsilon_b - 1)(1 - \epsilon_3)}. \quad (3.21b)$$

Chapter 4

Results

4.1 Steady State and Spasing Condition

One of the aims of our work is to determine if exists or not a steady state for the electric field created by the gain-assisted nanoshell in the emission regime. For this reason we look for the steady state solutions of system 3.21 (i.e. when all the time derivatives are set to zero). Using the normalization defined at the end of chapter 3, we can write $p_1 = E_0 - p_3 - (1 - \rho^3)p_2$. Consequently, the system of equations to solve is

$$p_1 = E_0 - p_3 - (1 - \rho^3)p_2, \quad (4.1a)$$

$$q_1 = \frac{1}{2}(\epsilon_b - \epsilon_h^*)p_1^*, \quad (4.1b)$$

$$q_2 = (1 - \epsilon_m)(p_1 + p_2), \quad (4.1c)$$

$$\sigma = -(1 - \epsilon_m)p_2. \quad (4.1d)$$

As a result of solving the system above, we obtain a relation between the dipole moment outside the nanoshell and the probe field.

$$p_3 = \frac{(\epsilon_m - \epsilon_3)(\epsilon_h + 2\epsilon_m) + \rho^3(\epsilon_3 + 2\epsilon_m)(\epsilon_h - \epsilon_m)}{(2\epsilon_m + \epsilon_h)(2\epsilon_3 + \epsilon_m) + 2\rho^3(\epsilon_m - \epsilon_h)(\epsilon_3 - \epsilon_m)} E_0 \quad (4.2)$$

Equation 4.2 can be written as

$$p_3 \alpha_{DEN} = \alpha_{NUM} E_0, \quad (4.3)$$

where

$$\alpha_{DEN} = (2\epsilon_m + \epsilon_h)(2\epsilon_3 + \epsilon_m) + 2\rho^3(\epsilon_m - \epsilon_h)(\epsilon_3 - \epsilon_m) \quad (4.4)$$

and

$$\alpha_{NUM} = (\epsilon_m - \epsilon_3)(\epsilon_h + 2\epsilon_m) + \rho^3(\epsilon_3 + 2\epsilon_m)(\epsilon_h - \epsilon_m) \quad (4.5)$$

In order to look for SPASER emission, we have to look for solutions that exist when the probe field E_0 is set to zero, which means that the right hand side of equation 4.3 is equal to zero. The only possible solution is $p_3 = 0$ for common dielectrics. However, when using gain materials in the core, the polarizability can become singular, its denominator $\alpha_{DEN} = 0$ allowing a solution with $p_3 \neq 0$ when $E_0 = 0$. This requirement of α_{DEN} enables us to find a relation between the permittivity in the core and the permittivity of the metal which can only be achieved with a gain medium.

$$\epsilon_h = \epsilon_m \frac{2(\epsilon_m - \epsilon_{out}) a_1^3 - 2(2\epsilon_{out} + \epsilon_m) a_2^3}{2(\epsilon_m - \epsilon_{out}) a_1^3 + (2\epsilon_{out} + \epsilon_m) a_2^3} = F(\omega) \quad (4.6)$$

Observe that we called as $F(\omega)$ to the expression for the permittivity within the core in the steady state obtained by solving the whole dynamical system of equations, which includes the shape of the particle through the boundary conditions. The same permittivity is also determined by using the dynamical equation for the population inversion 3.20b, and is given by expression 4.7.

$$\epsilon_h = \epsilon_b - \frac{\epsilon_h''(\omega_{21}) \tilde{N} \Delta [2(\omega - \omega_{21}) - i\Delta]}{4(\omega - \omega_{21})^2 + \Delta^2 \left[1 - \frac{\epsilon_h''(\omega_{21}) \tau_1 |p_1|^2}{2} \right]} \quad (4.7)$$

The procedure to obtain equation 4.7 is well explained in Appendix A. Since equations 4.6 and 4.7 describe the same permittivity, then the expression below is true.

$$\epsilon_b - \frac{\epsilon_h''(\omega_{21})\tilde{N}\Delta [2(\omega - \omega_{21}) - i\Delta]}{4(\omega - \omega_{21})^2 + \Delta^2 \left[1 - \frac{\epsilon_h''(\omega_{21})\tau_1|p_1|^2}{2}\right]} = F(\omega) \quad (4.8)$$

Equation 4.8 can be written as

$$\frac{-\epsilon_h''(\omega_{21})}{4(\omega - \omega_{21})^2 + \Delta^2 \left[1 + \frac{\epsilon_h''(\omega_{21})\tau_1|p_1|^2}{2}\right]} = \frac{F(\omega) - \epsilon_b}{\tilde{N}\Delta [2(\omega - \omega_{21}) - i\Delta]}. \quad (4.9)$$

Note that the left hand side of equation 4.9 is real, while the right hand side is complex. Equation 4.9 enables us to state two equations, one for the real parts and one for the imaginary parts. Let $F(\omega)$ be $F(\omega) = F'(\omega) + iF''(\omega)$. The imaginary contribution results in an expression to determine the spasing frequency, ω_{sp} .

$$2(\omega_{sp} - \omega_{21})F''(\omega_{sp}) + \Delta(F'(\omega_{sp}) - \epsilon_b) = 0 \quad (4.10)$$

Equation formed by equating the real parts is the following:

$$\frac{-\epsilon_h''(\omega_{21})}{4(\omega_{sp} - \omega_{21})^2 + \Delta^2 \left[1 - \frac{\epsilon_h''(\omega_{21})\tau_1|p_1|^2}{2}\right]} = \frac{2(\omega_{sp} - \omega_{21})(F'(\omega_{sp}) - \epsilon_b) - F''(\omega_{sp})\Delta}{\tilde{N}\Delta [4(\omega_{sp} - \omega_{21})^2 + \Delta^2]}. \quad (4.11)$$

Note that the right side of equation 4.11 does not depend on $\epsilon_h''(\omega_{21})$ and $|p_1|$. This means that the right hand side of the equation works for any value of $\epsilon_h''(\omega_{21})$ and $|p_1|$, including $\epsilon_h'''(\omega_{sp})$ and $|p_1| = 0$, where ω_{sp} is the frequency at the threshold. Therefore, the following equation is valid

$$\frac{\epsilon_h''(\omega_{21})}{4(\omega_{sp} - \omega_{21})^2 + \Delta^2 \left[1 - \frac{\epsilon_h''(\omega_{21})\tau_1|p_1|^2}{2}\right]} = \frac{\epsilon_h'''(\omega_{sp})}{4(\omega_{sp} - \omega_{21})^2 + \Delta^2}. \quad (4.12)$$

Using this last, we can deduce an equation that determines the spaser threshold, $\epsilon_h'''(\omega_{sp})$, by equating the right hand part of equation 4.12 with the right hand side of equation 4.11:

$$\epsilon_h'''(\omega_{sp}) = -\frac{2(\omega_{sp} - \omega_{21})(F'(\omega_{sp}) - \epsilon_b) - \Delta F''(\omega_{sp})}{\tilde{N}\Delta}. \quad (4.13)$$

Finally, from equation 4.12 we obtain an expression that shows the dependency of $|p_1|^2$ on the electric permittivity of the core,

$$|p_1|^2 = \frac{2}{\tau_1 \Delta^2} [4(\omega_{sp} - \omega_{21})^2 + \Delta^2] \frac{\epsilon_h'''(\omega_{sp}) - \epsilon_h''(\omega_{21})}{\epsilon_h''(\omega_{21})\epsilon_h'''(\omega_{sp})}. \quad (4.14)$$

In the non-linear steady state, the previous equation tells us how big is the magnitude of the dipole moment in the core depending on how many gain we have in the system. Observe that the gain level in the system, $\epsilon_h''(\omega_{21})$, must be greater than the gain threshold, $\epsilon_h'''(\omega_{sp})$, otherwise $|p_1|^2$ would be negative and would have no physical meaning. There is also another solution for equation 4.14, when $\epsilon_h'''(\omega_{sp}) = \epsilon_h''(\omega_{21})$, $|p_1|^2 = 0$ that means there is no electric field emitted inside the core and therefore there is no electric field all over the space. Observe that since we have a single line of emission in a given frequency, then we have a SPASER behavior of the system.

The results we obtained until this point were compared with the ones derived by D. G. Baranov on his article where he studies the same nanoshell system we study, and he deduced the same conclusions as us[26]. Baranov obtains the same SPASER behavior in the non-linear steady state for the nanoshell system. Nevertheless, he didn't analyzed the dynamics of the system nor the stability of this solution.

4.2 Dynamical Result

We used a computational method to recreate the time evolution of the plasmonic field inside the core until times around 6000 ns. We also varied the gain level by making it equal and bigger than the gain threshold. The following graphs are composed by two parts. In the top section, we can see the time evolution of the population inversion denoted by a purple line, and the progress in time of the emission of intensity in the core represented by a green shape. The bottom section shows the time development of the real and imaginary components of the electric

field inside the core, represented by a black and yellow line, respectively. The spasing frequency is marked with a vertical black line.

Figure 4.1 portrays the predicted trivial solution of equation 4.14, i.e. $|p_1|^2 = 0$ due to $\epsilon_h^{nth}(\omega_{sp}) = \epsilon_h''(\omega_{21})$. As we can see, at the spasing frequency the intensity never reaches a different value than zero. We can also note that the spasing frequency acts as an upper limit for the field emission. The time evolution of $\Re(E_1)$ and $\Im(E_1)$ conveys there is no steady state since they are always changing. Observe the emission occurs not only on a single frequency but on a narrow range.

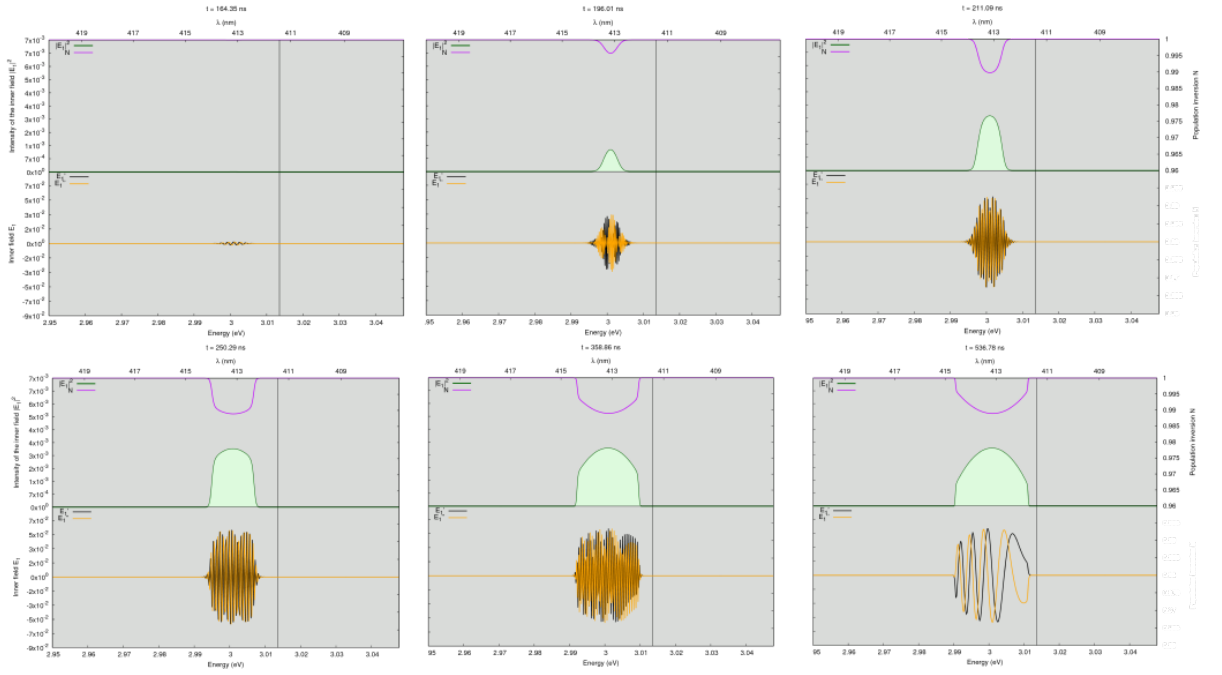


Figure 4.1: Time evolution of the system when $\epsilon_h^{nth}(\omega_{sp}) = \epsilon_h''(\omega_{21})$.

Figure 4.2 shows the time evolution of the system when the gain level is greater than the gain threshold. Note there is emission not only at the spasing frequency but in a narrow range around it. The spasing frequency does not match with the frequency where the higher emission takes place but is close to it. Since the range of wavelength emission is around 6 nm, then for practical purposes we can talk about a SPASER. However, again we don't have a steady state. Thus we can't define permittivities for the metal and the gain material. Which means the time evolution obtained by the numerical method does not fit to the result predicted by the analytical method; the system never reaches the steady state. Instead, the system reaches a dynamical solution.

This shows that there is a family of solutions that cannot be described through a steady state analysis because while it produce a steady state in the physical measurables (i.e. the intensity of the field), they are characterized by an eternal oscillation of the fields and the polarizarion involved.

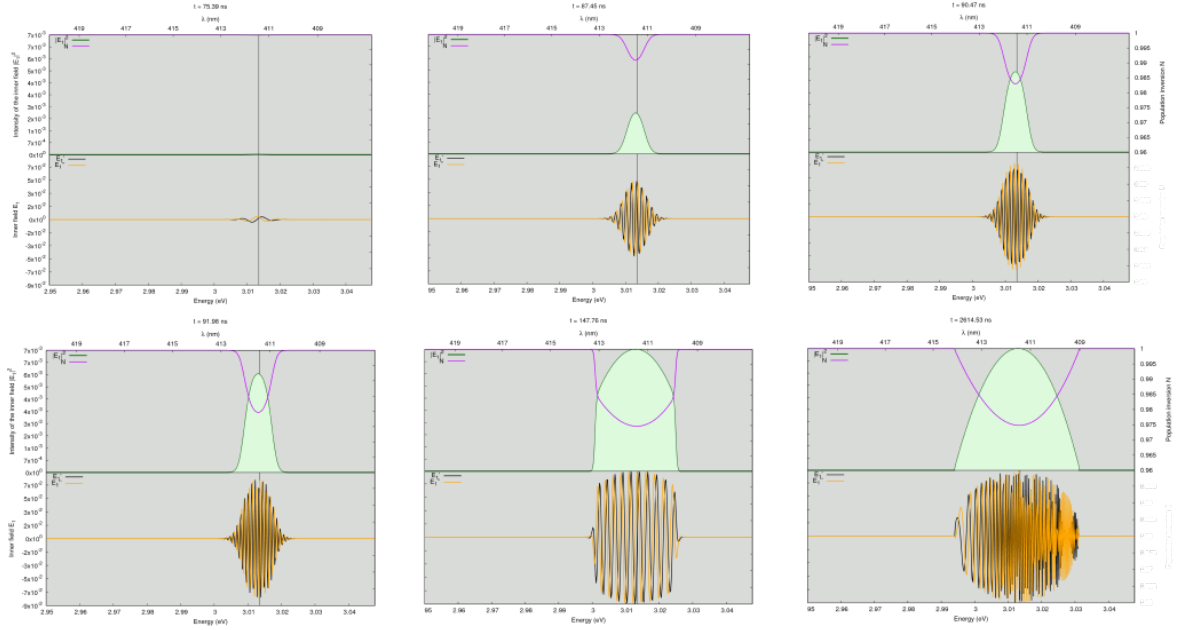


Figure 4.2: Time evolution of the system when $\epsilon_h^{nth}(\omega_{sp}) > \epsilon_h''(\omega_{21})$.

This does not mean that the solution discussed previously do not exist, but indicates that it could be related to a very small domain of initial conditions and therefore be experimentally unrealizable.

4.3 Conclusions

The analytical description of the nanoshell gain-assisted system portrays there is a line of emission for a given frequency, that we called spasing frequency, in the non-linear steady state. This result shows a SPASER behavior of the system when it is filled with more gain than the one given by the expression for the gain threshold. The analytical solution was compared with the article of D. Baranov and there is an agreement between both works since they predict the same SPASER behavior in the steady state. However, as we proceed to analyze the numerical result for

the equations that give shape to the system, we find that, as the time goes by, the steady state is not reached by the nanoshell, and that the intensity emission not occurs in a single frequency but in a range of frequencies close by the analitically calculated spasing frequency.

In conclusion, we have demonstrated that the system allows a dynamical solution that cannot be found using conventional steady state methods and is, to our knowledge, passed unnoticed until now. Also, our preliminary results in terms of stability of the solution seems to suggest that the steady state is a point only attainable within a restricted range of initial conditions. This kind of points are called repulsive points. If the system start from different initial conditions apart from this range, then the system won't be able to evolve to the steady state. As a further investigation, we are interested in an extensive dynamical characterization which will allow us to determine if the steady state is a repulsive point. If this is proven to be true, this would mean that the new dynamical solution we have found is the only one possible to observe experimentally.

Appendices

Appendix A

Gain Medium Electric Permittivity

Inside the core, the permittivity can be obtained from equations 3.20a, 3.20b and 3.9c deduced from the Optical-Bloch formalism and considering it as a two-level system. Since we are interested on the permittivity in the non-linear steady state, $d/dt = 0$, the equations to work with are the listed below. We also introduce $\tau_2 = 2/\Delta$.

$$\left[i(\omega - \omega_{21}) + \frac{1}{\tau_2} \right] q_1 = \frac{iN\epsilon_h''(\omega_{21})}{2\tau_2} p_1^* \quad (\text{A.1})$$

$$N - \tilde{N} = \Im\{q_1 p_1\} \tau_1 \quad (\text{A.2})$$

From equation A.1 we determine q_1 and q_1^* .

$$q_1 = \frac{N\Delta\epsilon_h''(\omega_{21})}{2[2(\omega - \omega_{21}) - i\Delta]} p_1^* \quad (\text{A.3})$$

$$q_1^* = \frac{N\Delta\epsilon_h''(\omega_{21})}{2[2(\omega - \omega_{21}) + i\Delta]} p_1 \quad (\text{A.4})$$

From the radial component of equation 3.9c, that describes the polarization density inside the core, we obtain the following expression.

$$P_1 = \epsilon_0 (\chi_b p_1 - 2q_1^*) \quad (\text{A.5})$$

We introduce q_1^* in equation A.5.

$$P_1 = \epsilon_0 \left[\chi_b - \frac{N\Delta\epsilon_h''(\omega_{21})}{2(\omega - \omega_{21}) + i\Delta} \right] p_1 \quad (\text{A.6})$$

Now it is easy to identify the relative electric permittivity inside the core, composed by gain material and background dielectric since $\epsilon_h = 1 + \chi_h$ and $\epsilon_b = 1 + \chi_b$.

$$\epsilon_h(\omega) = \epsilon_b - \frac{N\Delta\epsilon_h''(\omega_{21})}{2(\omega - \omega_{21}) + i\Delta} \quad (\text{A.7})$$

Let's calculate $\Im\{q_1 p_1\}$. Observe that

$$q_1 p_1 = \frac{N\Delta\epsilon_h''(\omega_{21})|p_1|^2 [2(\omega - \omega_{21}) + i\Delta]}{2 [4(\omega - \omega_{21})^2 + \Delta^2]} \quad (\text{A.8})$$

then

$$\Im\{q_1 p_1\} = \frac{N\Delta\epsilon_h''(\omega_{21})|p_1|^2}{2 [4(\omega - \omega_{21})^2 + \Delta^2]} \quad (\text{A.9})$$

Replacing the previous result on the expression for the population inversion, equation A.2 and after some algebra, we derive an expression for N .

$$N = \frac{\tilde{N} [4(\omega - \omega_{21})^2 + \Delta^2]}{4(\omega - \omega_{21})^2 + \Delta^2 \left[1 - \frac{\tau_1 \epsilon_h''(\omega_{21}) |p_1|^2}{2} \right]} \quad (\text{A.10})$$

Finally, we inject equation A.10 in equation A.7 and we obtain the non-linear steady state relative electric permittivity in the core.

$$\epsilon_h = \epsilon_b - \frac{\tilde{N} \Delta \epsilon_h''(\omega_{21}) [2(\omega - \omega_{21}) - i\Delta]}{4(\omega - \omega_{21})^2 + \Delta^2 \left[1 - \frac{\tau_1 \epsilon_h''(\omega_{21}) |p_1|^2}{2} \right]} \quad (\text{A.11})$$

Appendix B

Transition Frequency Condition

In the steady state, the electric permittivity in the core (gain material and background dielectric) is well described by a “single Lorentzian emission line shape” centered at the transition frequency between energy levels 2 and 1, ω_{21} :

$$\epsilon_h(\omega) = \epsilon_b - \frac{\epsilon_h''(\omega_{21})\Delta}{2(\omega - \omega_{21}) + i\Delta}, \quad (\text{B.1})$$

if we are interested precisely on the permittivity of the core in the spasing frequency, i.e. the spaser threshold, $\epsilon_h^{th}(\omega_{sp})$, what we have is:

$$\epsilon_h^{th}(\omega_{sp}) = \epsilon_b - \frac{\epsilon_h''(\omega_{21})\Delta}{2(\omega_{sp} - \omega_{21}) + i\Delta}; \quad (\text{B.2})$$

let $\epsilon_h^{th}(\omega_{sp}) = \epsilon_h'^{th}(\omega_{sp}) + i\epsilon_h''^{th}(\omega_{sp})$. Thus

$$\epsilon_h'^{th}(\omega_{sp}) + i\epsilon_h''^{th}(\omega_{sp}) = \epsilon_b - \frac{\epsilon_h''(\omega_{21})\Delta}{2(\omega_{sp} - \omega_{21}) + i\Delta}. \quad (\text{B.3})$$

The previous equation splits into two, one for the real part and one for the imaginary. The equality of the imaginary parts is the following:

$$\epsilon_h''(\omega_{sp}) = \frac{\epsilon_h''(\omega_{21})\Delta^2}{4(\omega_{sp} - \omega_{21})^2 + \Delta^2}. \quad (\text{B.4})$$

From the previous result we can deduce an expression for the transition frequency, ω_{21} , i.e. an expression that tells us what should be the magnitude of ω_{21} in order to have a Lorentzian shape of the permittivity at the threshold.

$$\omega_{21} = \omega_{sp} \pm \frac{\Delta}{2} \sqrt{\frac{\epsilon_h''(\omega_{21})}{\epsilon_h''(\omega_{sp})} - 1} \quad (\text{B.5})$$

If we take the negative sign in the previous equation, we get an expression for ω_{21} closer to the center of the plasmonic resonance, ω_{sp} . So we choose the negative sign for convenience.

$$\omega_{21} = \omega_{sp} - \frac{\Delta}{2} \sqrt{\frac{\epsilon_h''(\omega_{21})}{\epsilon_h''(\omega_{sp})} - 1} \quad (\text{B.6})$$

The transition frequency must be positive, then $\epsilon_h''(\omega_{21})/\epsilon_h''(\omega_{sp})$ needs to be greater than 1, this means that $\epsilon_h''(\omega_{21})$ should be more negative than $\epsilon_h''(\omega_{sp})$.

Bibliography

- [1] Kittel, C. (2005). *Introduction to Solid State Physics*. Eighth Edition. John Wiley & Sons, Inc.
- [2] Cathey, A. (2016). *Spaser Instability in Gain-Assisted Silver Nanoshell* (Undergraduate thesis). Universidad San Francisco de Quito USFQ: Quito.
- [3] Ashcroft, N. & Mermin N. (1976). *Solid State Physics*. Saunders College Publishing: Philadelphia.
- [4] Chipouline, A., Sugavanam, S., Fedotov, V. & Nikolaenko, A. (2012). "Analytical model for active metamaterials with quantum ingredients", *J.Opt.* 14, 114005.
- [5] Veltri, A. & Aradian, A. (2012). "Optical response of a metallic nanoparticle immersed in a medium with optical gain", *Physical Review B*, vol. 85, no. 11.
- [6] Whatmore. (2005). "Nanotechnology: what is it? Should we be worried?", *Nanotechnology Perceptions*, vol. 1.
- [7] El Naschie, S. (2006). "Nanotechnology for the developing world", *Elsevier*.
- [8] Maier, S. (2007). *Plasmonics: Fundamentals and Applications*. Springer.
- [9] Street, A., et al. (2014). *Nanotechnology Applications of Clean Water*. Second Edition. William Andrew: Oxford.
- [10] Baruah, S. & Dutta, J. (2009). "Nanotechnology applications in pollution sensing and degradation in agriculture: a review", *Environmental Chemistry Letters*, 7:191 204.
- [11] Nie, S., et al (2007). "Nanotechnology Applications in Cancer", *Annual Review of Biomedical Engineering*, 9:257 88.

- [12] Atwater, H. (2007). "The Promise of Plasmonics", *Scientific American*, vol. 296, no. 4.
- [13] Novotny, L. & Hecht, B. (2006). *Principles of Nano-Optics*. First Edition. Cambridge University Press: New York.
- [14] Abbe, E. (1906). *Gesammelte Abhandlungen*. No. v. 2 in *Gesammelte Abhandlungen*, Gustav Fischer.
- [15] Brongersma, M. & Kik, P. (2007). "Surface Plasmon Nanophotonics", *Springer series in optical sciences*, vol. 131, p.1, 2007.
- [16] Bohm, D. & Pines, D. (1953). "A Collective Description of Electron Interactions: III. Coulomb Interactions in a Degenerate Electron Gas", *Physical Review*, vol. 92, no.3, p.609.
- [17] Ritchie, R. (1957). "Plasma Losses by Fast Electrons in Thin Films", *Physical Review*, vol. 106, no. 5, p. 874.
- [18] Pelton, M. & Bryant, G. (2013). *Introduction to Metal-Nanoparticle Plasmonics*. VOL. 5. John Wiley & Sons, Inc.
- [19] Brambring, J. & Raether, H. (1965). "Plasma Radiation from Thin Silver Foils Excited by Light", *Physical Review Letters*, vol. 15, no. 23, p. 882.
- [20] Polo, J., Mackay, T. & Lakhtakia, A. (2013). *Electromagnetic Surface Waves: A Modern Perspective*. Newnes.
- [21] Kreibig, U. & Zacharias, P. (1970). "Surface plasma resonances in small spherical silver and gold particles", *Zeitschrift für Physik*, vol. 231, no. 2, p. 128-143.
- [22] Jackson, J. (1998). *Classical Electrodynamics*. Wiley.
- [23] Kim, K. (2012). "Plasmonics: Principles and Applications", *Application of Surface Plasmon Resonance Based Metal Nanoparticles*.
- [24] Rivera, V., et al. (2014). *Collective Plasmon Modes in Gain Media: Quantum Emitters and Plasmonic Nanostructures*. Springer.
- [25] Bergman, D. & Stockman, M. (2003). "Surface plasmon amplification by stimulated emission of radiation: quantum generation of coherent surface plasmons in nanosystems", *Physical Review Letters*, vol. 90, no. 2.
- [26] Baranov, D., et al. (2013). "Exactly solvable toy model for surface plasmon amplification by stimulated emission of radiation", *Optics Express*, vol. 21, no. 9.